NANO LETTERS

2007
Vol. 7, No. 9
2645−2649

Temperature Dependence of the Raman Spectra of Graphene and Graphene Multilayers

I. Calizo,[†] A. A. Balandin,*[,†] W. Bao,[‡] F. Miao,[‡] and C. N. Lau[‡]

Nano-Device Laboratory, Department of Electrical Engineering, University of California—Riverside, Riverside, California 92521, and Department of Physics and Astronomy, University of California—Riverside, Riverside, California 92521

Received May 2, 2007; Revised Manuscript Received August 7, 2007

ABSTRACT

We investigated the temperature dependence of the frequency of *G* peak in the Raman spectra of graphene on Si/SiO_2 substrates. The micro-Raman spectroscopy was carried out under the 488 nm laser excitation over the temperature range from −190 to +100 °C. The extracted value of the temperature coefficient of *G* mode of graphene is $\chi = -0.016$ cm^{-1}/°C for the single layer and $\chi = -0.015$ cm^{-1}/°C for the bilayer. The obtained results shed light on the anharmonic properties of graphene.

Graphene, a two-dimensional honeycomb lattice of carbon atoms, exhibits rather unusual energy dispersion relations—the low-lying electrons in single-layer graphene behave like massless relativistic Dirac fermions with vanishing density of states at the Dirac point. Since the recent micromechanical isolation and measurements of graphene by Novoselov et al.,[1−2] it has attracted tremendous attention.[1−16] The Dirac spectrum in graphene is predicted to give rise to a number of phenomena such as quantum spin Hall effect,[4−6] enhanced Coulomb interaction,[7−11] and suppression of the weak localization.[12−13] It was recently discovered that graphene has clear signatures in the Raman spectroscopic microscopy,[14−16] which make this technique suitable for a quick inspection of the number of layers in graphene materials and identification of single-layer graphene.

Raman spectroscopy is a noninvasive technique, which was widely used to characterize the structural and electronic properties of the carbon-based materials such as carbon nanotubes (CNT),[17−20] diamond,[21−23] graphite,[24−25] and diamond-like carbons.[26−27] Ferrari et al.[14] have demonstrated that micro-Raman spectroscopy can be used for unambiguous and high-throughput identification of the exact number of the graphene layers. Both *G* and 2*D* bands can be used to monitor the number of layers.[14−16] Such an ability is essential for the material characterization and graphene−structure optimization for the proposed device applications. Raman spectroscopy was also instrumental in the investigation, which suggested a breakdown of the adiabatic Born−Oppenheimer approximation in graphene by demonstrating the stiffening of the Raman *G* peak.[28]

In this letter, we present a study of the temperature dependence of Raman spectrum of graphene. Such study is important for further understanding of the fine structure and properties of the material such as atomic bonds, thermal expansion, specific heat, and thermal conductivity. An additional motivation is the use of the micro-Raman spectroscopy for materials identification because the change of the phonon frequency with temperature and laser power may present serious difficulties in the spectrum analysis and peak assignment. The temperature variations of the Raman spectrum in CNT have been studied in detail.[17−20] The frequency downshift with increasing temperature has been observed for all Raman modes of CNTs including the radial breathing mode (RBM) and the tangential stretching mode. Although it is known that the temperature dependence of Raman spectra is due to the anharmonic terms in the lattice potential energy, the exact physical mechanism still awaits detailed description even for such a well-researched material as CNT. The commonly used descriptions of the temperature dependence of Raman spectrum of the carbon-based materials are the elongation of the C−C bond due to thermal expansion or anharmonic coupling of phonon modes.[19] To the best of our knowledge, the temperature dependence of graphene has not been reported yet.

The samples investigated in this work have been obtained by the micromechanical cleavage of bulk Kish graphite, i.e., the same technique that allowed the graphene isolation for the first time.[1−2] Single- and bilayer graphene pieces were mechanically exfoliated and transferred to the silicon wafers,

* Corresponding author. E-mail: balandin@ee.ucr.edu.
[†] Nano-Device Laboratory, Department of Electrical Engineering.
[‡] Department of Physics and Astronomy.

10.1021/nl071033g CCC: $37.00
Published on Web 08/25/2007

which were covered with 300 nm of thermal oxide. We identified the single- and bilayer graphenes by the color inference in the optical microscope: the single-layer graphene is nearly transparent, and the bilayer appears as very pale purple (see Figure 1a). The graphene pieces were imaged by the atomic force microscopy (AFM) to ensure the uniformity of the layer. Figure 1b shows a typical AFM image of the graphene layers on a silicon substrate, which were used for this study. After AFM quality control, the graphene layers on silicon substrates were transferred under the optical microscope connected to the Raman spectrometer (Figure 1c shows the actual spots from which the Raman data were collected).

The measurements have been carried out using a Renishaw micro-Raman spectrometer.[29−30] All spectra were excited with visible (488 nm) laser light and collected in the backscattering configuration. The spectra were recorded with a 1800 lines/mm grating. We have used a 50× objective to focus the excitation laser light on the right spot of the graphene samples. The sample temperature was controlled by a cold−hot cell operated using a liquid nitrogen source. A special precaution was taken to avoid local heating of the samples by the excitation laser. To achieve this, all measurements were carried out at low excitation power. The power on top of the cold−hot cell window was below 4.8 mW and, correspondingly, much smaller on the sample surface. The power density on the cold−hot cell window or sample surface was measured using an Orion laser power meter. The estimated accuracy of the cell temperature control was ±0.1 °C.

Figure 2 shows a typical spectrum from a single graphene layer on silicon over the measured spectral range. The most notable features of the spectrum are the *G* peak at 1580 cm^{-1}, which corresponds to the E_{2g} mode, and a relatively wide band around 2700 cm^{-1}, which we refer to as 2*D* following the terminology introduced by Ferrari et al.[14] The 2*D* band (historically referred to as *G*′) is an overtone of the *D* band. The so-called disorder-induced *D* band is frequently observed in carbon materials at ∼1350 cm^{-1}. The *D* band has been attributed to in-plane A_{1g} (LA) zone-edge mode, which is silent for the infinite layer dimensions but becomes Raman active for small layers or layers with substantial number of defects through the relaxation of the phonon wave-vector selection rules.[31] To verify the number of graphene layers in the produced samples, we analyzed the variation of the 2*D* band (see Figure 3). The observed spectrum variation is in agreement the previously reported data.[14−16] The distinctively different Raman signatures of the single-, bi-, and multilayers of graphene allowed us to accurately monitor the number of layers in our samples and make sure that the temperature dependence is measured for the single-layer or bilayer graphene.

The temperature dependence of the *G* peak position, measured in the range from $T = -190$ °C (−160 °C) to $T = +100$ °C for a single-layer and bilayer graphene, is shown in Figure 4 a,b. The increasing temperature leads to the red shift of the *G* peak. The general trend is clearly observed over the examined temperature range. Some data dispersion

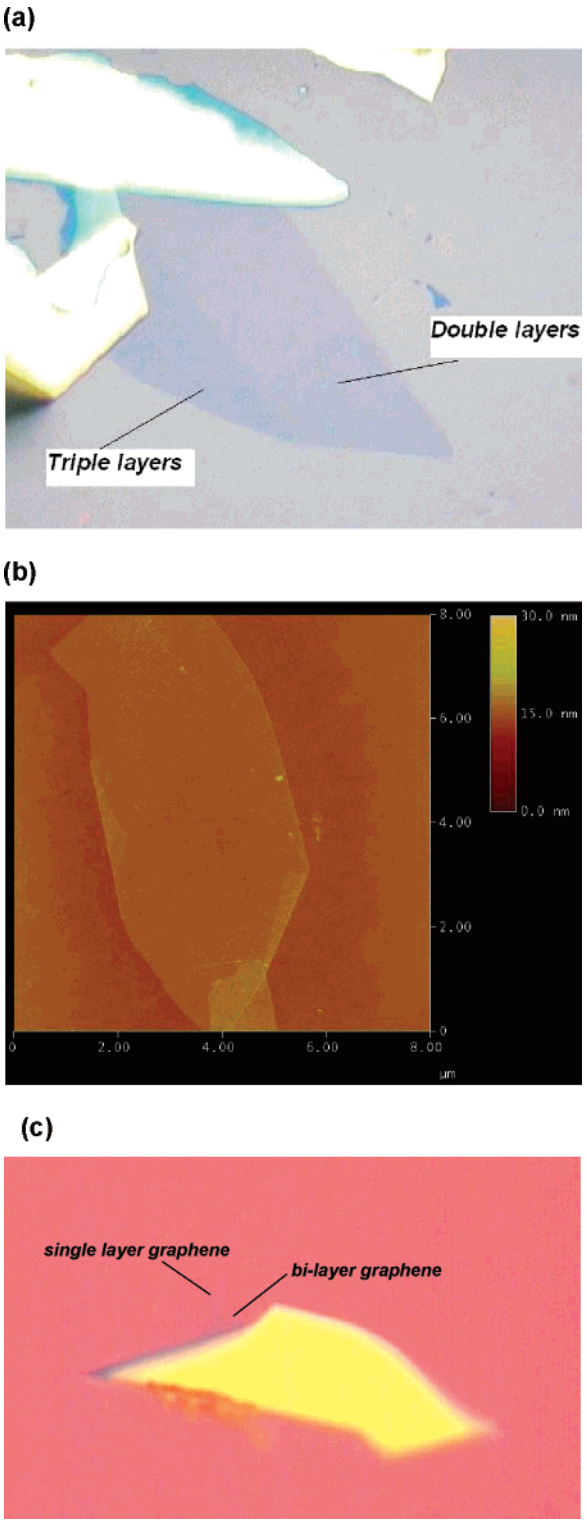

Figure 1. (a) Optical microscopy image of graphene layers on silicon substrates with the 300 nm thick layer of thermal silicon oxide; (b) atomic force microscopy micrograph of the few-layer graphene flake on silicon substrate; (c) optical image of the graphene layers under the microscope connected to the Raman spectrometer indicating the spots where the temperature-dependent data were taken.

for the *G* peak position can be attributed to several factors. They include a low excitation power on the sample surface after the additional attenuation through the cold−hot cell window and the drift of the laser spot along the graphene

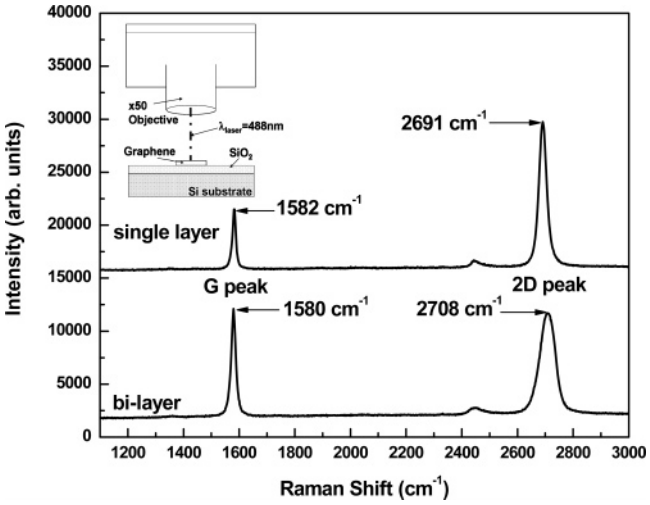

Figure 2. Room-temperature Raman spectra from the single- and bilayer graphene on silicon excited at 488 cm^{-1}. The *G* peak at 1582 cm^{-1} and 2*D* band at 2700 cm^{-1} are clearly seen. Inset: experimental setup arrangement.

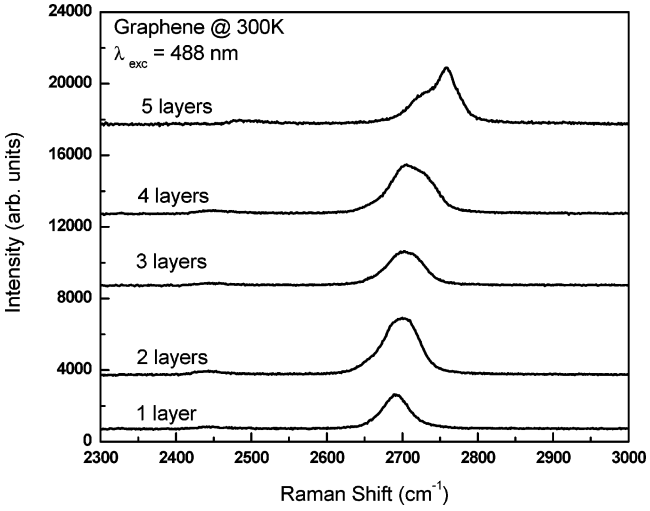

Figure 3. Room-temperature Raman spectrum of the graphene flake in the 2*D* band spectral region. Note distinctive features of the spectrum from the single-layer graphene and multiple layers of graphene excited by a 488 nm laser. The spectra were used to verify the number of layers.

surface after the temperature change. Although small, the drift may result in errors due to the high sensitivity of the *G* peak to the number of graphene layers and the presence of defects. A similar magnitude data scatter even for the room-temperature *G* peak position was observed and discussed by Gupta et al.[15] The measurements were repeated several times to verify the reproducibility.

The temperature dependence of the *G* mode frequency shift in graphene can be represented by the following relation:

$$\omega = \omega_0 + \chi T \qquad (1)$$

where ω_o is the frequency of *G* mode when temperature *T* is extrapolated to 0 K and χ is the first-order temperature coefficient, which defines the slope of the dependence. The second-order term is expected to appear only at the high

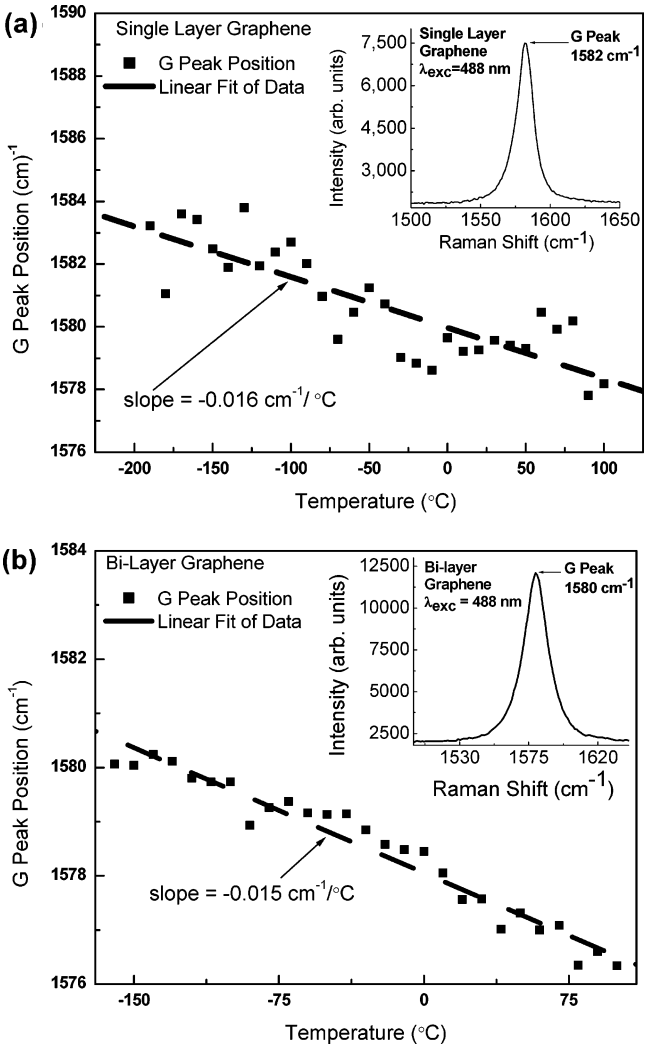

Figure 4. Temperature dependence of the *G* peak frequency for the single- (a) and bilayer (b) graphene. The insets show the shape of *G* peak. The measured data were used to extract the temperature coefficient for *G* peak.

temperature, which is in line with the observations made for other carbon materials. The temperature coefficient χ of the *G* mode determines the frequency shift of the *G* mode when the temperature of the sample increases by 1 °C (or K). The extracted negative value for a single-layer graphene is $\chi = -(1.62 \pm 0.20) \times 10^{-2}$ cm^{-1}/K. Similar measurements carried out for the graphene bilayer gave the value of $\chi = -(1.54 \pm 0.06) \times 10^{-2}$ cm^{-1}/K. The extrapolated ω_o values are 1584 and 1582 cm^{-1} for the single- and bilayer graphene, correspondingly.

The change of the phonon frequency with temperature is a manifestation of the anharmonic terms in the lattice potential energy, which is determined by the anharmonic potential constants, the phonon occupation number, and the thermal expansion of the crystal.[32] The temperature effects can be roughly divided into the "self-energy" shift due to the anharmonic coupling of the phonon modes and the shift contribution due to the thermal expansion of the crystal. Although the thermal expansion by itself is also a result of the anharmonicity, its physical mechanism is different and related to the change of the force constants of the material

Table 1. Temperature Coefficient for Carbon-Based Materials[a]

sample	χ (cm^{-1}/K)	λ_{laser} (nm)	heating method	temperature range (K)	reference
single-layer graphene	−0.0162	488	external	83−373	this work
bilayer graphene	−0.0154	488	external	113−373	this work
DWCNT	−0.022	647, 568, 515, 482	laser	180−320	Bassil et al.[20]
D-CNT	−0.023	632.8	laser	420−770	Huang et al.[17]
C-CNT	−0.028	632.8	laser	420−770	Huang et al.[17]
A-C	−0.027	632.8	laser	420−770	Huang et al.[17]
SWNT	−0.0189	514	external	299−773	Raravikar et al.[18]
CHOPG	−0.028	514.5	laser	286−647	Tan et al.[25]
HOPG	−0.011	514.5	laser	286−647	Tan et al.[25]
diamond	−0.012	406.7	external	300−1900	Zouboulis et al.[22]

[a] All data are for the *G* peak except for diamond, which is for the diamond peak at ~1332 cm^{-1}.

with volume. Thus, the measured frequency change $\Delta\omega = \omega - \omega_o$ can be written as

$$\Delta\omega \equiv (\chi_T + \chi_V)\Delta_T = \left(\frac{d\omega}{dT}\right)_V \Delta T + \left(\frac{d\omega}{dV}\right)_T \Delta V = \left(\frac{d\omega}{dT}\right)_V \Delta T + \left(\frac{d\omega}{dV}\right)_T \left(\frac{d\omega}{dT}\right)_P \Delta T \quad (2)$$

Here we defined χ_T to be the "self-energy" shift due to the direct coupling of the phonon modes (sometimes also referred to as "pure" or "intrinsic" temperature effect) and χ_V as the shift due to the thermal expansion induced volume change. Because our measurements have been carried out at constant pressure rather than constant volume, both contributions are reflected in the extracted values of the temperature coefficient and it has to be interpreted as the sum of both contributions, i.e., $\chi = \chi_T + \chi_V$.

It is illustrative to compare the temperature effects in a single-layer graphene with those in other carbon-based materials such as diamond, CNT, and graphite. Table 1 presents a detail summary and comparison of the temperature dependence of the *G* peak in different carbon materials. One should note that, in some studies, the temperature variation was very small because the temperature was not externally controlled (when the sample is heated or cooled in the cold cell) but rather changed locally through the variation of the excitation laser power. Overall, the rate of the *G* band shift with the temperature, χ, in graphene is somewhat lower than that for the single-wall carbon nanotubes (SWCNT), which was found to be -0.019 to -0.029 cm^{-1}/K.[17−18,20,33] The temperature coefficient for the highly oriented pyrolytic graphite (HOPG) was found to be $\chi = -0.011$ cm^{-1}/K.[25] From the known thermal expansion coefficient for HOPG, the authors argued that the temperature coefficient χ for HOPG is mostly due to the "self-energy" contribution and not to the thermal expansion, i.e., $\chi \approx \chi_T$.[24−25] The latter was explained by the fact that the thermal expansion of graphite crystals mainly occurs along the *c*-axis and has a small effect of the frequency of the in-plane mode.

The carbon (^{12}C) implantation of HOPG samples at ambient temperature led to noticeable increase in the absolute value of the thermal coefficient of the resulting CHOPG samples to $\chi = -0.028$ cm^{-1}/K.[24−25] The latter value is closer to what has been measured for "active" carbon (A-C)[17] and various CNT samples (see Table 1). One should remember that CNT samples of regular purity contain significant portion of other forms of carbon. Our data suggest that the absolute value of the temperature coefficient for the bilayer graphene is smaller than that for the single-layer graphene. This may be an indication of the trend for the $|\chi|$ decrease with the increasing number of layers and the approach to the χ value for the high-quality HOPG. Further investigation of graphene samples produced by different techniques and theoretical analysis of the anharmonic processes are needed for the final conclusions.

The measured room-temperature full width at half-maximum (fwhm) of the *G* peak of the single-layer and bilayer graphene is 13.5 and 18.2 cm^{-1}, respectively. It is comparable to the fwhm of 12 and 17 cm^{-1} reported for HOPG and CHOPG by Tan et al.[25] Naturally, these values are much larger than those for diamond, which are in the range from 1.1 to 2.9 cm^{-1} as summarized in ref 23. It is interesting to note that we did not observe the dependence of fwhm in the single-layer or bilayer graphene on temperature in the examined range of temperatures beyond the experimental uncertainty. This is in contrast with the temperature dependence of fwhm for diamond[21−23] but in line with the report for the *G* mode of HOPG.[25]

Because the examined graphene layers were supported by the silicon wafers with 300 nm of thermal oxide (SiO_2), one may consider a possible effect of the substrate on the obtained values of χ for the graphene *G* mode. One cannot exclude the role of the substrate on the Raman signatures, and it deserves a separate investigation. At the same time, we believe that the presence of the substrate does not strongly affect our conclusions about the thermal coefficients χ for the following reasons. The measured *G* band at 1582 cm^{-1} is made up of the optical phonons with the long wavelength. The *G*-band optical phonons in graphene represent the in-plane vibrations because the E_{2g} symmetry of this band restricts the motion of the atoms to the plane of the carbon atoms.[34] The out-of-plane vibrations (ZO phonons), which were not studied in this paper, have the zone-center frequency around 861 cm^{-1}.[35−36] According to the first-principles calculations,[36] the out-of-plane vibrations in graphene are not coupled to the in-plane motion, which define the *G* band

spectra position. The out-of-plane vibrations are expected to be more susceptible to the substrate influence. Thus, it is reasonable to assume that the measured temperature coefficients for the *G* band are mostly the characteristics of the graphene layers rather than the substrate-induced property. This conclusion is supported by the fact that the Raman peaks in suspended graphene were found to be similar to those on Si/SiO_2 substrates[14] and that the temperature coefficient for the phonon peak in silicon is different (4.7×10^{-5} °C^{-1})[36] from the one we determined for graphene. The thermal expansion coefficient for silicon and SiO_2 are low ($\sim 2.6 \times 10^{-6}$ °C^{-1}), and the thermal expansion of the substrate over the examined temperature range of ~290 °C does not induce substantial stress to the graphene layers. The previous studies of the thermal coefficients for Raman peaks in CNTs (see Table 1) tacitly made similar assumptions about a weak influence of the substrate on the measured χ values for CNTs.

In summary, we reported the first experimental investigation of the temperature dependence of the frequency the *G* peak in the Raman spectra of graphene on Si/SiO_2 substrates. The extracted value of the temperature coefficient of the *G* mode is $\chi = -(1.6 \pm 0.2) \times 10^{-2}$ cm^{-1}/K for the single-layer graphene and $\chi = -(1.5 \pm 0.06) \times 10^{-2}$ cm^{-1}/K for the bilayer graphene. The experimental uncertainties, which are likely related to the low excitation power on the sample surface, drift of the laser spot, and sensitivity of the *G* peak to the presence of defects, do not allow us to make a final conclusion about the difference between the thermal coefficients for the single- and bilayer graphene. The temperature coefficient for *G* mode in graphene was compared with the data for other carbon materials. The obtained results shed light on the anharmonic properties of graphene and can be used for the accurate interpretation of Raman spectra from graphene layers.

Acknowledgment. The work by I.C. and A.A.B. has been supported, in part, by the DARPA−SRC funded MARCO Center on Functional Engineered Nano Architectonics (FENA). A.A.B. also acknowledges the National Science Foundation (NSF) CAREER Award.

References

(1) Novoselov, K. S.; Geim, A. K.; Morozov, S. V.; Jiang, D.; Zhang, Y.; Dubonos, S. V.; Grigorieva, I. V.; Firsov, A. A. *Science* **2004**, *306*, 666.
(2) Novoselov, K. S.; Geim, A. K.; Morozov, S. V.; Jiang, D.; Katsnelson, M. I.; Grigorieva, I. V.; Dubonos, S. V.; Firsov, A. A. *Nature* **2005**, *438*, 197.
(3) Zhang, Y. B.; Tan, Y. W.; Stormer, H. L.; Kim, P. *Nature* **2005**, *438*, 201.
(4) Abanin D. A.; Lee P. A.; Levitov L. S. *Phys. Rev. Lett.* **2007**, *98*, 156801, cond-mat/0611062.
(5) Kane, C. L.; Mele, E. J. *Phys. Rev. Lett.* **2005**, *95*, 226801.
(6) Kane, C. L.; Mele, E. J. *Phys. Rev. Lett.* **2005**, *95*, 146802.
(7) Khveshchenko, D. V. *Phys. Rev. B* **2006**, *74*, 161402.
(8) Hwang E. H.; Sarma S. D. cond-mat/0610561.
(9) Ezawa, M. *Physica E* **2007**, http://dx.doi.org/10.1016/j.physe.2007.06.038, cond-mat/0609612; Wang X-F. **2006**, cond-mat/0611635.
(10) Katsnelson, M. I. *Phys. Rev. B* **2006**, *74*, 201401.
(11) Miao, F.; Wijeratne, S.; Zhang, Y.; Coskun, U.; Bao, W.; Lau, C. N. *Science* **2007**, cond-mat/0703052.
(12) Novoselov, K. S.; McCann, E.; Morozov, S. V.; Fal'ko, V. I.; Katsnelson, M. I.; Zeitler, U.; Jiang, D.; Schedin, F.; Geim, A. K. *Nat. Phys.* **2006**, *2*, 177.
(13) Morozov, S. V.; Novoselov, K. S.; Katsnelson, M. I.; Schedin, F.; Ponomarenko, L. A.; Jiang, D.; Geim, A. K. *Phys. Rev. Lett.* **2006**, *97*, 016801.
(14) Ferrari, A. C.; Meyer, J. C.; Scardaci, V.; Casiraghi, C.; Lazzeri, M.; Mauri, F.; Piscanec, S.; Jiang, D.; Novoselov, K. S.; Roth, S.; Geim, A. K. *Phys. Rev. Lett.* **2006**, *97*, 187401.
(15) Gupta, A.; Chen, G.; Joshi, P.; Tadigadapa, S.; Eklund, P. C. *Nano Lett.* **2006**, *6*, 2667.
(16) Graf, D.; Molitor, F.; Ensslin, K.; Stampfer, C.; Jungen, A.; Hierold, C.; Wirtz, L. *Nano Lett.* **2007**, *7*, 238.
(17) Huang, F.; Yue, K. T.; Tan, P.; Zhang, S.-L.; Shi, Z.; Zhou, X.; Gu, Z. *J. Appl. Phys.* **1998**, *84*, 4022.
(18) Raravikar, N. R.; Keblinski, P.; Rao, A. M.; Dresselhaus, M. S.; Schadler, L. S.; Ajayan, P. M. *Phys. Rev. B* **2002**, *66*, 235424.
(19) Ci, L.; Zhou, Z.; Song, L.; Yan, X.; Liu, D.; Yuan, H.; Gao, Y.; Wang, J.; Liu, L.; Zhou, W.; Wang, G.; Xie, S. *Appl. Phys. Lett.* **2003**, *82*, 3098.
(20) Bassil, A.; Puech, P.; Tubery, L.; Bacsa, W.; Flahaut, E. *Appl. Phys. Lett.* **2006**, *88*, 173113.
(21) Herchen, H.; Cappelli, M. A. *Phys. Rev. B* **1991**, *43*, 11740.
(22) Zouboulis, E. S.; Grimsditch, M. *Phys. Rev. B* **1991**, *43*, 12490.
(23) Liu, M. S.; Bursill, L. A.; Prawer, S.; Beserman, R. *Phys. Rev. B* **2000**, *61*, 3391.
(24) Tan, P. H.; Deng, Y.; Zhao, Q. *Phys. Rev. B* **1998**, *58*, 5435.
(25) Tan, P. H.; Deng, Y.; Zhao, Q.; Cheng, W. *Appl. Phys. Lett.* **1999**, *74*, 1818.
(26) Ferrari, A. C.; Robertson, J. *Phys. Rev. B* **2000**, *61*, 14095.
(27) Ferrari, A. C.; Robertson, J. *Phys. Rev. B* **2001**, *64*, 075414.
(28) Pisana, S.; Lazzeri, M.; Casiraghi, C.; Novoselov, K. S.; Geim, A. K.; Ferrari, A. C.; Mauri, F. *Nat. Mater.* **2007**, *6*, 198.
(29) Alim, K. A.; Fonoberov, V. A.; Shamsa, M.; Balandin, A. A. *J. Appl. Phys.* **2005**, *97*, 024313.
(30) Alim, K. A.; Fonoberov, V. A.; Balandin, A. A. *Appl. Phys. Lett.* **2005**, *86*, 053103.
(31) Vidano, R. P.; Fischbach, D. B.; Willis, L. J.; Loehr, T. M. *Solid State Commun.* **1981**, *39*, 341.
(32) Postmus, C.; Ferraro, J. R.; Mitra, S. S. *Phys. Rev.* **1968**, *174*, 983.
(33) Jorio, A.; Fantini, C.; Dantas, M. S. S.; Pimenta, M. A.; Souza Filho, A. G.; Samsonidze, Ge. G.; Brar, V. W.; Dresselhaus, G.; Dresselhaus, M. S.; Swan, A. K.; Unlu, M. S.; Goldberg, B. B.; Saito, R. *Phys. Rev. B* **2002**, *66*, 115411.
(34) Tuinstra, F.; Koenig, J. L. *J. Chem. Phys.* **1970**, *53*, 1126.
(35) Mounet, N.; Marzari, N. **2004**, cond-mat/0412643.
(36) Falkovsky, L. A. **2007**, cond-mat/0702409.
(37) Perichon, S.; Lysenko, V.; Remaki, B.; Barbier, D.; Champagnon, B. *J. Appl. Phys.* **1999**, *86*, 4700.

NL071033G